Dalton Transactions

Accepted Manuscript

This article can be cited before page numbers have been issued, to do this please use: M. T. Weller and A. Dennington, *Dalton Trans.*, 2016, DOI: 10.1039/C6DT03602C.

ROYAL SOCIETY OF CHEMISTRY

www.rsc.org/dalton

View Article Online
DOI: 10.1039/C6DT03602C

Journal Name

ARTICLE

Synthesis and structure of pseudo-three dimensional hybrid iodobismuthate semiconductors

Received 00th January 20xx,
Accepted 00th January 20xx

DOI: 10.1039/x0xx00000x

www.rsc.org/

A. J. Dennington[a] and M. T. Weller[a]

The synthesis, structures and semiconducting properties of three isostructural, piperazinium-cation based iodobismuthates, $[NH_2(CH_2)_4NH_2][BiI_4]_2.4H_2O$, $[CH_3NH(CH_2)_4NH_2][BiI_4]_2.3H_2O$ and $[CH_3NH(CH_2)_4HNCH_3][BiI_4]_2.2H_2O$, are reported. The materials have pseudo-three dimensional structures consisting of infinite chains formed from edge/face sharing $[BiI_6]$ octahedra with short interchain I…I interactions of <3.8Å. The materials have band gaps of ~1.9-2.0 eV and show variable optoelectronic properties based on the degree of methylation of the templating piperazinium ring-based organic species and the accordingly associated level of solvation in the structure.

Introduction

The emergence of metal halide perovskite photovoltaic materials over the last few years has ignited much attention towards discovering new semiconducting, organic-inorganic hybrid materials[1-3]. Lead-based materials, in particular methylammonium lead iodide (MAPI), currently dominate the field and now demonstrate solar cell efficiencies to over 22%[4]. Although commercially viable efficiencies have been validated for perovskite cells, they typically exhibit limited stability leading to concerns over for long term operation in a solar cell. Studies have been undertaken to discern and combat the issue of instability of hybrid perovskite materials when exposed to light (and/or) air;[5-7] some reports suggest an inherent thermodynamic instability of the structures resulting in a spontaneous decomposition process to the respective lead and organo-cationic halide precursor species[8]. A further key concern with these materials is that they contain toxic lead.

There is, therefore, an urgent need to discover new functional optoelectronic materials. These will need to reproduce the impressive optoelectronic properties of the lead halide perovskites but replace the toxic lead and have improved materials stability in device processing and in long-term deployment. It has been proposed that the required semiconducting properties of the lead halide perovskites derive from the fundamental electronic structure[9]. In particular, partially oxidised post transition metals with filled $5s^2$ or $6s^2$ orbitals have been shown to produce shallow defects and a dispersed valence band. As a result, the most promising metal cation candidates for further study are considered to be Sn^{2+}, Bi^{3+} and Sb^{3+}. Much initial work focussed on the isovalent substitution of Pb^{2+} by Sn^{2+} [10-12]. However, Sn^{2+} compounds generally undergo rapid oxidation by air and decomposition through reaction with moisture[13, 14].

Bismuth is an environmentally friendly, non-toxic alternative with the potential to form materials exhibiting the required optoelectronic properties. Bulk bismuth is relatively expensive compared to lead but for thin film technologies, requiring ~4-12g/m^2 of absorber material, the cost with bismuth, at under \$1/m^2, is reasonable in terms of overall device cost.

Work on semiconducting metal halide materials has been extended to double perovskite systems, with general formula $A_2BB'X_6$(X=halide) with B'= Sn, Pb. Recently, bismuth-based halide double perovskites Cs_2AgBiX_6(X = Cl, Br) have been reported as exhibiting comparable, though larger, band gaps to their $(MA)PbX_3$ analogues[15-18]. Another route to novel hybrid semiconducting materials is to search outside of the confines of perovskite structures while aiming to maintain high structural and optoelectronic connectivity. Typically iodometallate, X = I, structures are favoured targets over other halide systems as they tend to possess smaller band gaps and lower carrier effective masses[17]. However, substitution of Pb^{2+} by Bi^{3+}, with X = I, normally yields zero- (0D) and one-dimensional (1D) iodobismuthate structures. Previously reported iodobismuthate materials demonstrate a large diversity of anionic substructures[19, 20], built from linked $[BiI_6]$ octahedra including vertex sharing, edge-sharing and face-sharing motifs. Anionic units range from discrete 0D units in $[BiI_6]^{3-}$ to $[Bi_8I_{30}]^{4-}$ motifs[21-35], through 1D chain structures[22, 36-40], including the commonly found $[BiI_4]^-_n$ and $[BiI_5]^{2-}_n$; with one reported 2D extended network, $[Bi_{2/3}I_4]^{2-}_n$[41]. To date well over 50 iodobismuthate materials have been described but three-dimensional structural, and, therefore, optoelectronic connectivity has proved elusive.

[a] The University of Bath – Department of Chemistry, Bath, United Kingdom of Great Britain and Northern Ireland BA2 7AY

† Footnotes relating to the title and/or authors should appear here.

Electronic Supplementary Information (ESI) available: [details of any supplementary information available should be included here]. See DOI: 10.1039/x0xx00000x

View Article Online
DOI: 10.1039/C6DT03602C

Experimental section

General

Our exploration of hybrid iodobismuthate materials has led to the discovery of three new, isostructural materials $[NH_2(CH_2)_4NH_2][BiI_4]_2.4H_2O$, $[CH_3NH(CH_2)_4NH_2][BiI_4]_2.3H_2O$ and $[CH_3NH(CH_2)_4HNCH_3][BiI_4]_2.2H_2O$. These isostructural materials have pseudo-three dimensional structures, reminiscent of the perovskite structure, where links between $[BiI_4^-]_n$ chains occur through short I---I interactions These materials also exhibit tuneable properties through the substitution of the piperazinium cation ring and, in turn, via control of solvate water molecules in the structures.

Synthetic

Crystals of the 1,4-dipiperazinium iodobismuthate tetrahydrate $[NH_2(CH_2)_4NH_2][BiI_4]_2.4H_2O$ (Compound **1**) were obtained through hydrothermal reaction of $BiCl_3$ (0.2mmol, 98%(dry wt.), Alfa Aesar), piperazine (0.15mmol, >98%, Fluka), HI (0.5ml, 57wt%, no stabiliser, Sigma-Aldrich) in deionised water (6ml). Reactants placed in a 25ml Teflon-lined vessel, sealed in a steel autoclave and heated at 140°C for 24h; with a controlled ramp up rate of 1°C/min and ramp down rate of 0.1°C/min. After filtration and ethanol wash, a pure phase of prismatic red block crystals of compound **1** (0.147g) was obtained.

Deep red crystals of 1-methyl-1,4-dipiperazinium iodobismuthate trihydrate, $[CH_3NH(CH_2)_4NH_2][BiI_4]_2.3H_2O$, (Compound **2**) were synthesised utilising identical conditions and procedure as described for **1** with the exception of a change of the organic templating agent to 1-methylpiperazine (0.15mmol, 99%, Sigma-Aldrich) and an increased volume of HI (0.75ml 57wt%, no stabiliser, Sigma-Aldrich); these reaction conditions yielded a pure phase of millimetre-sized crystals (0.130g).

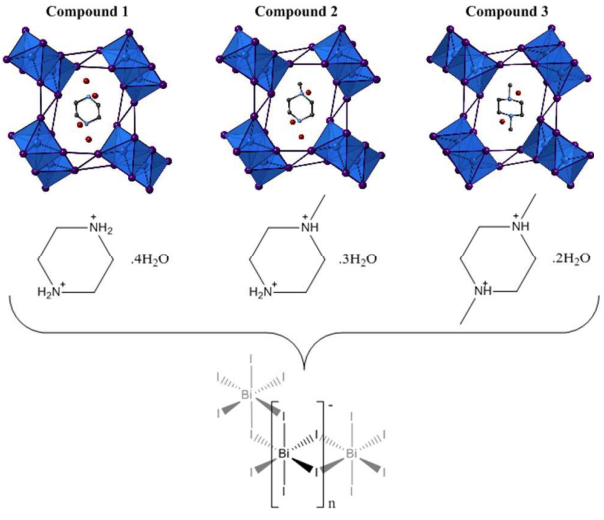

Fig. 1 A schematic illustration of the *a*-axis views of Compounds **1-3**

Deep red crystals of 1,4-dimethyl-1,4-dipiperazinium iodobismuthate dihydrate, $[CH_3NH(CH_2)_4HNCH_3][BiI_4]_2.2H_2O$ (Compound **3**), were attained through the hydrothermal reaction of $BiCl_3$ (0.4mmol, 98%(dry wt.), Alfa Aesar), 1,4-dimethylpiperazine (0.15mmol, 98%, Alfa Aesar), HI (1ml, 57wt%, no stabiliser, Sigma-Aldrich) in deionised water (6ml). Reactants were placed in a 25ml Teflon-lined vessel, sealed in a steel autoclave and heated at 170°C for 24h; with a controlled ramp up rate of 1°C/min and ramp down rate of 0.1°C/min. After filtration and ethanol wash a pure phase of crystals of Compound **3** (0.206g) was obtained.

Results and discussion

General

The structures of compounds **1-3** were solved from single crystal X-ray diffraction data (see ESI) All three compounds, $[NH_2(CH_2)_4NH_2][BiI_4]_2.4H_2O$, $[CH_3NH(CH_2)_4NH_2][BiI_4]_2.3H_2O$ and $[CH_3NH(CH_2)_4HNCH_3][BiI_4]_2.2H_2O$, crystallise in the monoclinic space group $P2_1/c$ with lattice parameters shown in Table 1. The materials are iso-structural and consist of infinite chains of the stoichiometry $[BiI_4^-]_n$ with short interchain I---I contacts. The voids delineated by the chains and inter-chain contacts are occupied by the organic cations and water molecules in a manner reminiscent of the perovskite structure, Figure 1.

	1a (150K)	1b (RT)	2a (150K)	2b (RT)	3a (150K)	3b (RT)
a (Å)	7.3508(2)	7.4697(3)	7.5434(2)	7.6488(4)	7.7293(2)	7.7971(3)
b (Å)	13.0215(4)	13.1773(7)	13.0515(5)	13.1532(8)	13.0336(3)	13.0868(5)
c (Å)	13.9875(3)	13.9099(6)	13.6716(5)	13.7033(7)	13.4990(4)	13.5505(6)
β (°)	94.588(2)	95.109(4)	96.347(3)	96.481(5)	97.955(3)	97.925(4)
V (Å^3)	1334.57(2)	1363.72(11)	1337.76(8)	1369.83(13)	1346.81(6)	1369.48(10)

Table 1 Unit cell parameters for Compounds 1-3 at RT and 150K data collections

Stability and dehydration

Thermogravimetric analysis of compound **1** displays a weight loss of 4.2% at temperature range 70 - 110°C corresponding to the desolvation of all four water molecules from the hydrated structure. In the same way, the tri- and di-hydrate structures of Compounds **2** & **3** exhibit dehydration steps with weight losses of 3.7% and 2.0% respectively; in close agreement with the weight percentage contributions to the unit cell. All three dehydrated structures show thermal stability to approximately 250°C before undergoing degradation (Figure S1-3 – see ESI).

Crystal structure analysis

In compound **1**, the dipiperazinium dications counterbalance the charge of the anionic $[BiI_4^-]_n$ chains and are located within channels extending through the *a*-axis of the structure in parallel with the sublattice. Neutral water molecules fully occupy four sites within the structure.

In Compound **2** the organic cation is disordered, adopting one of two possible orientations, and as a result the steric effect of the methyl group partially blocks the occupancy of two of the water molecule positions; previously fully occupied in

View Article Online
DOI: 10.1039/C6DT03602C

Compound **1**. That is, these water molecule sites become half-filled due to the methyl group of the locally orientated 1-methyl-dipiperazinium cations occupying and so impeding the spaces. This reduces the overall hydration level in Compound **2** to give a trihydrate hybrid iodobismuthate, $[CH_3NH(CH_2)_4NH_2][BiI_4]_2.3H_2O$. Following this behaviour and trend, in compound **3**, the methyl groups of the positionally ordered 1,4-dimethyldipiperazinium cation precludes occupation of both these water molecule sites occupied in Compound **1** and this results in the formation of a dihydrate, $[CH_3NH(CH_2)_4HNCH_3][BiI_4]_2.2H_2O$. Elongated thermal parameters on the nitrogen and methyl carbon atoms in this structure indicates some possible local conformational disorder of the organic cation in the structure.

The changes to the cation and associated degree of solvation result in subtle but important changes to the anionic sub-lattice. The $[BiI_4^-]_n$ chains are formed from edge sharing individual $[BiI_6]$ octahedra, leading to 4 bridging and 2 terminal cis-related iodine atoms. The bismuth atom is slightly displaced from a central position in the $[BiI_6]$ octahedron with the shortest Bi-I interactions observed to the two terminal iodine atoms. This behaviour is in agreement with observations for other iodobismuthate materials possessing similar 1D $[BiI_4^-]_n$ chain motifs[38-40, 42, 43]. The range of Bi-I bond lengths within the octahedra decreases from compound **1** to compound **3** suggesting an increased overall regularity of the

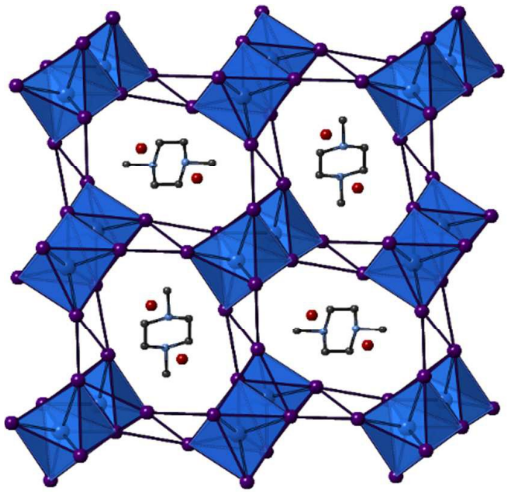

Fig. 2 View down the a-axis of Compound 3 highlighting the inter chain I….I interactions

octahedra.

Interchain I---I interactions extend the anionic network along both the *b*- and *c*-axes of all three compounds; this can be considered as producing a degree of 3D connectivity in the materials and a potential route for electronic interactions between the $[BiI_4^-]_n$ chains. Three I---I pathways repeat regularly along the chain axis with all iodine atoms involved in interactions with adjacent chains; the longest of these being a terminal-terminal I---I interaction and the shortest two edge iodine to terminal iodine interactions. Lengths of these interactions range from 3.76-4.44Å in the structures and the average distance of the interchain interactions decreases, 4.14Å→4.09Å→4.00Å (150K), through Compounds **1**-**3** respectively. The shortest interchain interaction is observed to exhibit minor variation through the structures 3.76Å→3.77Å→3.78Å (150K). In the series Compound **1** to Compound **3** the interchain Bi…Bi distances increase by an average of 0.05 Å as Bi-I-Bi bond angles increase beyond the octahedral angles; from 90.5°→91.9°→93.2° (150 K).

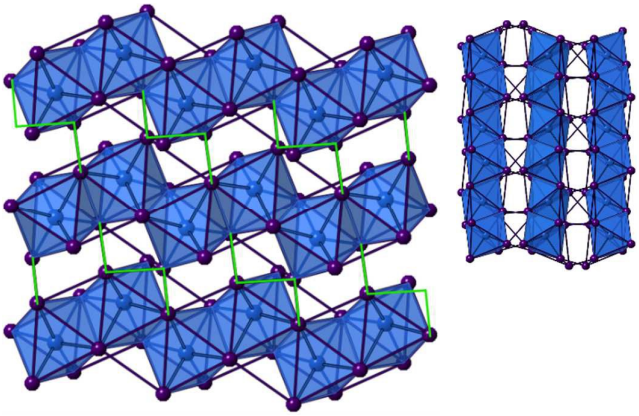

Fig. 3 Left: b-axis view of the anionic 1D network present in all compounds with interchain interactions highlighted (green). Right: (top)- c-axis view of the anionic network observed in all structures

In summary progressing from piperazinium-based, Compound **1**, through 1-methylpiperazinium-based, Compound **2**, to 1,4-dimethyldipiperazinium-based, Compound **3**, causes systematic changes within the 1D anionic chain network. These trends are observed as an extension of the distances between bismuth atom positions within the chain; Bi…Bi distances to intrachain next-but-one octahedra steadily increase 7.35Å→7.54Å→7.73Å (150 K). This behaviour is accompanied by an increased level of distortion within the chains as Bi-I-Bi angles extend from 90.5°→93.2°. Simultaneously the average lengths of I---I interchain interactions decrease which increases the pseudo-3D nature of the materials. Interchain Bi…Bi distances decrease in tandem, with the average of the three closest interchain Bi…Bi distances falling from 9.20Å→9.10Å→8.85Å (150K) from Compound **1** to Compound **3**. Hydrogen bonding between the solvent water molecules and the protonated amine groups and/or the iodide ions of the $[BiI_4^-]_n$ chains is likely to be present in all three compounds. Note that while hydrogen positions with the water molecules were modelled in all three structures, the true molecular orientations of the molecules could not be determined in these heavy atom compounds.

Optical absorption measurements

Optical absorption spectra (250-800nm) were collected for pure phases of Compounds **1-3** (Figure 4). Each compound shows absorption across the majority of the visible region consistent with their observed dark red colouration. The

View Article Online
DOI: 10.1039/C6DT03602C

absorption edge onset was determined from Tauc plots as 550, 560 and 575 nm which assuming a direct band gap for the strong absorption coefficients gives E_g values of 2.00eV, 1.95eV and 1.92eV for Compounds **1**-**3** respectively (Figure S4 – see ESI). These shifts could be attributed to the trend seen in decreasing interchain I---I distances and, therefore, increasing pseudo 3D-connectivity within these structures. Additional

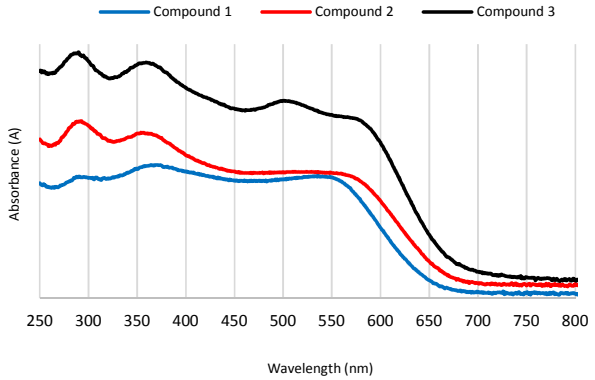

Fig. 4 UV/Vis spectra of Compounds 1-3 (10 wt% mixtures in $BaSO_4$)

absorption peak features can be observed in the spectra for all three compounds at ~290nm(4.3eV) and ~360nm (3.4eV). Compound **3** also has an additional absorption peak at ~500nm(2.5eV). Previous studies of iodobismuthate structures have shown similar distinct bands that have been attributed to electronic transitions from the HOMO Bi(6p) orbital to the LUMO Bi(5p) orbitals [25, 38].

Conclusions

In summary, three new, pseudo-3D piperazinium-based hybrid iodobismuthate materials have synthesised and structurally characterised. All three structures have been shown by thermogravimetric analysis to undergo dehydration processes while maintaining the integrity of the bismuth-iodide framework and semiconducting properties. Preliminary variable temperature SXD/PXRD studies indicate that the dehydration is reversible in these materials. This behaviour should be of interest in respect of depositing thin-films of these materials as it indicates that sample degradation, as seen with the lead halide perovskites, will not occur. Increased methylation of the templating piperazinium ring, tied with a decreased level of solvate within the structure, has been shown to result in average shortening of the I---I interactions between 1D $[BiI_4^-]_n$ chains in the anionic network. Correspondingly, analysis by optical absorption indicates a shift in absorption edge in relation to this trend; with all three materials demonstrating band gap energies of ~1.9-2.0eV; estimated from the intercept of the maximum angle of the absorption edge. Although this value is too large for use as a highly efficient absorber materials in a single junction cell architecture, their use in tandem solar cell architectures can still be considered. The pseudo-three dimensional features of the structures of these materials, and the ability to tune them through variations in the geometry of the templating organic cation signifies a further step towards obtaining highly functional yet less toxic stable perovskite-like hybrid absorber materials for future use in solar technologies.

Acknowledgements

The authors would like to thank Dr Mary F. Mahon for assistance with the single crystal X-ray crystallography. AJD would like to thank EPSRC for DTA studentship support.

Notes and references

‡ *Crystal data* for 1a: $C_4H_{20}N_2O_4Bi_2I_8$, M = 1593.41, monoclinic, space group P21/c, a = 7.3508(2), b = 13.0215(4), c = 13.9875(3) Å, β = 94.588(2)°, V = 1334.57(2)Å^3, Z = 4, crystal size: 0.506x0.232x0.114mm, T = 150.01(10)K, ρ_{calc} = 3.965gcm^{-3}, μ = 22.429mm^{-1}, 16574 reflections (4290 unique reflections), 91 parameters, 0 restraints, R1(all data) = 0.0446, wR2(all data) = 0.0889, GooF = 1.145, Further details available from CCDC 1496110**.**

Crystal data for 1b: $C_4H_{20}N_2O_4Bi_2I_8$, M = 1593.41, monoclinic, space group P21/c, a = 7.4697(3), b = 13.1773(7), c = 13.9099(6) Å, β = 95.109(4)°, V = 1363.72(11)Å^3, Z = 4, crystal size: 0.358x0.260x0.0.123mm, T = 292.0(2)K, ρ_{calc} = 3.880gcm^{-3}, μ = 21.950mm^{-1}, 8961 reflections (4208 unique reflections), 91 parameters, 0 restraints, R1(all data) = 0.0634, wR2(all data) = 0.1049, GooF = 1.044, Further details available from CCDC 1496109

Crystal data for 2a: $C_5H_{20}N_2O_3Bi_2I_8$, M = 1589.27, monoclinic, space group P21/c, a = 7.5434(2), b = 13.0515(5), c = 13.6716(5) Å, β = 96.347(3)°, V = 1337.76(5)Å^3, Z = 4, crystal size: 0.434x0.189x0.168mm, T = 149.95(10)K, ρ_{calc} = 7.890gcm^{-3}, μ = 22.371mm^{-1}, 14198 reflections (4214 unique reflections), 109 parameters, 0 restraints, R1(all data) = 0.0381, wR2(all data) = 0.0722, GooF = 1.158, Further details available from CCDC 1496112.

Crystal data for 2b: $C_5H_{20}N_2O_3Bi_2I_8$, M = 1589.27, monoclinic, space group P21/c, a = 7.6488(4), b = 13.1532(8), c = 13.7033(7) Å, β = 96.481(5)°, V = 1369.83(13)Å^3, Z = 4, crystal size: 0.413x0.176x0.176mm, T = 292.23(10)K, ρ_{calc} = 3.804gcm^{-3}, μ = 43.639mm^{-1}, 8333 reflections (4206 unique reflections), 109 parameters, 0 restraints, R1(all data) = 0.0590, wR2(all data) = 0.0970, GooF = 1.075, Further details available from CCDC 1496111

Crystal data for 3a: $C_6H_{20}N_2O_2Bi_2I_8$, M = 1585.43, monoclinic, space group P21/c, a = 7.7293(2), b = 13.0336(3), c = 13.4990(4) Å, β = 97.955(3)°, V = 1346.79(6)Å^3, Z = 4, crystal size: 0.300x0.215x0.181mm, T = 150.10(10)K, ρ_{calc} = 3.894gcm^{-3}, μ = 22.220mm^{-1}, 7814 reflections (4138 unique reflections), 91 parameters, 0 restraints, R1(all data) = 0.0402, wR2(all data) = 0.0788, GooF = 1.150, Further details available from CCDC 1496114.

Crystal data for 3b: $C_6H_{20}N_2O_2Bi_2I_8$, M = 1585.43, monoclinic, space group P21/c, a = 7.7971(3), b = 13.0868(5), c = 13.5505(6) Å, β = 97.925(4)°, V = 1369.48(9)Å^3, Z = 4, crystal size: 0.298x0.217x0.180mm, T = 286(9)K**,** ρ_{calc} = 3.830gcm^{-3}, μ = 21.851mm^{-1}, 8720 reflections (2879 unique reflections), 91 parameters, 0 restraints, R1(all data) = 0.0654, wR2(all data) = 0.0849, GooF = 1.021, Further details available from CCDC 1496113

View Article Online
DOI: 10.1039/C6DT03602C

Single crystal data for compounds 1-3 were collected on an Agilent Xcalibur four-circle diffractometer equipped with a fine-focus (Mo_{ka}) X-ray source and EosS2 CCD plate detector.

1. H. J. Snaith, *J. Phys. Chem. Lett.*, 2013, **4**, 3623-3630.
2. M. A. Green, A. Ho-Baillie and H. J. Snaith, *Nat. Photo.*, 2014, **8**, 506-514.
3. S. Kazim, M. K. Nazeeruddin, M. Gratzel and S. Ahmad, *Angew. Chem-Int. Ed.*, 2014, **53**, 2812-2824.
4. Research cell efficiency records, http://www.nrel.gov/ncpv/images/efficiency_chart.jpg (accessed July 2016)).
5. G. D. Niu, X. D. Guo and L. D. Wang, *J. Mat. Chem. A*, 2015, **3**, 8970-8980.
6. J. L. Yang, B. D. Siempelkamp, D. Y. Liu and T. L. Kelly, *ACS Nano*, 2015, **9**, 1955-1963.
7. Y. Han, S. Meyer, Y. Dkhissi, K. Weber, J. M. Pringle, U. Bach, L. Spiccia and Y. B. Cheng, *J. Mat. Chem. A*, 2015, **3**, 8139-8147.
8. A. M. Ganose, C. N. Savory and D. O. Scanlon, *J. Phys. Chem. Lett.*, 2015, **6**, 4594-4598.
9. R. E. Brandt, V. Stevanovic, D. S. Ginley and T. Buonassisi, *MRS Comm.*, 2015, **5**, 265-275.
10. N. K. Noel, S. D. Stranks, A. Abate, C. Wehrenfennig, S. Guarnera, A. A. Haghighirad, A. Sadhanala, G. E. Eperon, S. K. Pathak, M. B. Johnston, A. Petrozza, L. M. Herz and H. J. Snaith, *Energ. Environ. Sci.*, 2014, **7**, 3061-3068.
11. C. C. Stoumpos, C. D. Malliakas and M. G. Kanatzidis, *Inorg. Chem.*, 2013, **52**, 9019-9038.
12. M. Weiss, J. Horn, C. Richter and D. Schlettwein, *Phys. Stat. Solid. a-App. Mat. Sci.*, 2016, **213**, 975-981.
13. D. B. Mitzi, S. Wang, C. A. Feild, C. A. Chess and A. M. Guloy, *Sci.*, 1995, **267**, 1473-1476.
14. D. B. Mitzi, C. D. Dimitrakopoulos and L. L. Kosbar, *Chem. Mat.*, 2001, **13**, 3728-3740.
15. A. H. Slavney, T. Hu, A. M. Lindenberg and H. I. Karunadasa, *J. Amer. Chem. Soc.*, 2016, **138**, 2138-2141.
16. E. T. McClure, M. R. Ball, W. Windl and P. M. Woodward, *Chem. Mat.*, 2016, **28**, 1348-1354.
17. G. Volonakis, M. R. Filip, A. A. Haghighirad, N. Sakai, B. Wenger, H. J. Snaith and F. Giustino, *J. Phys. Chem. Lett.*, 2016, **7**, 1254-1259.
18. M. Filip, S. Hillman, A. Haghighirad, H. Snaith and F. Giustino, *J. Phys. Chem. Lett.*, 2579-2585.
19. L. M. Wu, X. T. Wu and L. Chen, *Coord. Chem. Rev.*, 2009, **253**, 2787-2804.
20. S. A. Adonin, M. N. Sokolov and V. P. Fedin, *Coord. Chem. Rev.*, 2016, **312**, 1-21.
21. A. M. Goforth, L. Peterson, M. D. Smith and H. C. zur Loye, *J. Solid State. Chem.*, 2005, **178**, 3529-3540.
22. W. H. Bi and N. Mercier, *Chem. Comm.*, 2008, 5743-5745.
23. A. M. Goforth, J. R. Gardinier, M. D. Smith, L. Peterson and H. C. Z. Loye, *Inorg. Chem. Comm.*, 2005, **8**, 684-688.
24. C. Hrizi, A. Samet, Y. Abid, S. Chaabouni, M. Fliyou and A. Koumina, *J. Mol. Struct.*, 2011, **992**, 96-101.
25. A. Samet, A. Ben Ahmed, A. Mlayah, H. Boughzala, E. K. Hlil and Y. Abid, *J. Mol. Struct.*, 2010, **977**, 72-77.
26. A. M. Goforth, M. A. Tershansy, M. D. Smith, L. Peterson, J. G. Kelley, W. J. I. DeBenedetti and H. C. zur Loye, *J. Amer. Chem. Soc.*, 2011, **133**, 603-612.
27. C. Feldmann, *J. Solid State. Chem.*, 2003, **172**, 53-58.
28. J. Heine, *Dalton Trans.*, 2015, **44**, 10069-10077.
29. H. Krautscheid, *Z. Anorg. Allge. Chem.*, 1995, **621**, 2049-2054.
30. H. Krautscheid, *Z. Anorg. Allge. Chem.*, 1999, **625**, 192-194.
31. S. A. Adonin, E. V. Peresypkina, M. N. Sokolov and V. P. Fedin, *Russ. J. Coord. Chem.*, 2014, **40**, 867-870.
32. H. Krautscheid, *Z. Anorg. Allge. Chem.*, 1994, **620**, 1559-1564.
33. K. Y. Monakhov, C. Gourlaouen, R. Pattacini and P. Braunstein, *Inorg. Chem.*, 2012, **51**, 1562-1568.
34. V. V. Sharutin, I. V. Egorova, N. N. Klepikov, E. A. Boyarkina and O. K. Sharutina, *Russ. J. Inorg. Chem.*, 2009, **54**, 1768-1778.
35. A. Okrut and C. Feldmann, *Z. Anorg. Allge. Chem.*, 2006, **632**, 409-412.
36. D. B. Mitzi and P. Brock, *Inorg. Chem.*, 2001, **40**, 2096-2104.
37. G. A. Mousdis, G. C. Papavassiliou, A. Terzis and C. P. Raptopoulou, *Z. Natur. Sec. B-a J. Chem. Sci.*, 1998, **53**, 927-931.
38. C. Hrizi, N. Chaari, Y. Abid, N. Chniba-Boudjada and S. Chaabouni, *Polyhedron*, 2012, **46**, 41-46.
39. S. Chaabouni, S. Kamoun and J. Jaud, *J. Chem. Cryst.*, 1997, **27**, 527-531.
40. N. A. Yelovik, A. V. Mironov, M. A. Bykov, A. N. Kuznetsov, A. V. Grigorieva, Z. Wei, E. V. Dikarev and A. V. Shevelkov, *Inorg. Chem.*, 2016, **55**, 4132-4140.
41. D. B. Mitzi, *Inorg. Chem.*, 2000, **39**, 6107-6113.
42. M. Erbe, D. Kohler and M. Ruck, *Z. Anorg. Allge. Chem.*, 2010, **636**, 1513-1515.
43. A. Gagor, M. Weclawik, B. Bondzior and R. Jakubas, *Crystengcomm*, 2015, **17**, 3286-3296.